Medium modifications of the ρ meson in nuclear photoproduction

F. Riek,[1,*] R. Rapp,[1,†] Yongseok Oh,[2,‡] and T.-S. H. Lee[3,§]
[1]*Cyclotron Institute and Physics Department, Texas A&M University, College Station, Texas 77843-3366, USA*
[2]*School of Physics and Energy Sciences, Kyungpook National University, Daegu 702-701, Korea*
[3]*Physics Division, Argonne National Laboratory, Argonne, Illinois 60439, USA*
(Received 9 March 2010; published 15 July 2010)

We extend our recent study of dilepton invariant-mass spectra from the decays of ρ mesons produced by photon reactions off nuclei. We specifically focus on experimental spectra as recently measured by the CLAS Collaboration at the Thomas Jefferson National Accelerator Facility using carbon and iron nuclei. Building on our earlier work, we broaden our description to a larger set of observables to identify sensitivities to the medium effects predicted by microscopic calculations of the ρ spectral function. We compute mass spectra for several target nuclei and study the spectral shape as a function of the three-momentum of the outgoing lepton pair. We also compute the so-called nuclear transparency ratio, which provides an alternative means (and thus consistency check) of estimating the ρ width in the cold nuclear medium.

DOI: 10.1103/PhysRevC.82.015202 PACS number(s): 21.65.Jk, 25.20.Lj, 14.40.Be

I. INTRODUCTION

The study of in-medium properties of vector mesons has been pursued vigorously in recent years. The restoration of the spontaneously broken chiral symmetry at high temperature and/or density predicts that hadron properties change when approaching pertinent phase changes: the spectral functions of chiral partners are believed to degenerate [1–4]. Precursor effects of chiral restoration may already occur in more dilute hadronic matter, where medium modifications can be computed in more controlled calculations using many-body techniques. How far such medium effects can be related to fundamental properties of the QCD phase transition(s) remains an open question. On the experimental side, electromagnetic probes (real and virtual photons) are very suitable because no significant distortions occur owing to strong initial- and/or final-state interactions with the nuclear medium. Invariant-mass spectra of dileptons in heavy-ion collisions (HICs) at the Super Proton Synchrotron (SPS) [5–7] clearly revealed the presence of medium modifications of the ρ-meson spectral function in the hot and dense medium. The most recent NA60 dimuon data [8] enable the average medium effect on the ρ meson to be quantified as an approximately threefold broadening relative to its free width with little (if any) mass shift [9,10]. This average, however, results from a time evolution of a hot and dense fireball encompassing hadron densities that vary by approximately a factor of 5 from the critical temperature ($T_c \simeq 175$ MeV) down to thermal freeze-out ($T_{\rm fo} \simeq 120$–130 MeV). Thus, the predictive power under such conditions requires not only a good knowledge of the time evolution of temperature and baryon density but also a well-constrained model for the in-medium physics figuring into the vector-meson spectral functions. More elementary reactions using a single-particle projectile directed on nuclear targets offer a valuable simplification of both aspects: (a) the nucleus provides a static medium (at zero temperature) and (b) the medium consists of nucleons only (rather than including a tower of mesonic and baryonic excitations). A further benefit is that medium effects induced by nucleons (baryons) were indeed identified as the more relevant one relative to mesons [10–13]. Although these features should, in principle, allow for a better theoretical control in the evaluation of medium effects, there is, of course, a price to pay: (i) the medium density is restricted to that of normal nuclear matter, $\varrho_0 = 0.16$ fm^{-3}, with significant density gradients owing to surface effects and (ii) the production mechanism is more involved (generally depending on the projectile) compared to an approximately thermal medium in ultrarelativistic HICs. Nevertheless, if the latter point can be addressed satisfactorily (e.g., by gauging the production process on proton targets), valuable information on medium effects is expected to emerge from the investigation of nuclear dilepton production experiments.

Dilepton spectra in elementary reactions were measured using both proton- and photon-induced production off nuclei. Using a 12-GeV proton beam at KEK, the E325 Collaboration reported a significant reduction in the ρ mass [14]. However, with a 1–3.5-GeV incident-energy photon beam at JLab, the CLAS Collaboration [15,16], using an absolutely normalized background subtraction procedure, found not a significant mass shift but rather a moderate broadening of the dilepton excess spectrum associated with ρ decays (cf. also Ref. [17] for two-pion production experiments on light nuclei).

As indicated above, the starting point for a theoretical description of these reactions is a realistic model for the elementary production process, $\gamma N \to e^+e^-N$, as studied by several authors [18–21]. In our previous study [22], we combined the meson-exchange model of Ref. [21] with an in-medium ρ propagator [10], which describes low-mass dilepton and photon spectra in HICs at the CERN-SPS [9]. The production amplitude was augmented by baryon resonance channels to ensure consistency with the medium effects in the ρ propagator. Using an average local-density approximation for the decay points of the ρ, this model was found to describe the

*friek@comp.tamu.edu
†rapp@comp.tamu.edu
‡yohphy@knu.ac.kr
§lee@phy.anl.gov

dilepton invariant-mass spectra off iron targets, as measured by the CLAS Collaboration, fairly well.

In this article, we improve and extend our previous work [22] in several respects. First, we refine our schematic model for estimating the density probed by the ρ meson by folding over a realistic density distribution (rather than using an average density), thereby accounting for momentum and density dependence of the decay rate. The improved description is compared to existing carbon and iron data, supplemented by predictions for several heavier targets to illustrate the sensitivity to medium effects when going up to uranium. We furthermore investigate the role of three-momentum cuts on the outgoing lepton pair as an additional means to enhance the observable medium modifications. Finally, we compute the so-called nuclear transparency ratio as an independent (and thus complementary) observable to obtain quantitative information on the in-medium width of the ρ meson by measuring how the absolute magnitude of the cross section depends on the nuclear mass number.

This paper is organized along the aforementioned lines. In Sec. II we briefly recall the main ingredients of our approach, the improvements, and the resulting density profiles probed by the ρ decays. In Sec. III we update the comparison to existing data (Sec. III A) and carry out the sensitivity studies with respect to the target (Sec. III B) and three-momentum (Sec. III C) dependence of the spectra, as well as the transparency ratio of the total yields (Sec. III D). We conclude in Sec. IV.

II. ρ PRODUCTION AND DECAY IN NUCLEI

We first recapitulate the main components of our model as constructed in Ref. [22]. The elementary photoproduction amplitude, for the process $\gamma p \to e^+e^- p$, is based on the meson-exchange model developed by two of us [21], which accounts for σ, f_2, π, and Pomeron t-channel exchange as well as nucleon s- and u-channel pole diagrams. This model gives a very good description of the total ρ production cross section for incoming photon energies $E_\gamma \geqslant 2.5$ GeV. Because the input spectrum used by the CLAS Collaboration at JLab contains photon energies down to $\sim$1 GeV, we extended the model by including s-channel baryon-resonance excitations. By implementing the same set of resonances (with the same coupling constants and form factors) that were used in the calculation of in-medium ρ spectral function [10,23], a good description of the low-energy part of the ρ-production cross section was found. The description of the angular distributions (which are forward dominated for t-channel exchanges) also improves because the resonance decays generate significant strength at large scattering angles. This provides a realistic starting point for the production mechanism on nuclear targets and establishes consistency between the production amplitude and the medium effects induced by the subsequent propagation of the ρ meson through the nucleus. In addition to direct resonance excitations, $\rho + N \to B^*$, the model for the in-medium ρ propagator includes the dressing of its two-pion cloud via nucleon-hole (NN^{-1}) and delta-hole (ΔN^{-1}) excitations. When translated into contributions to the $\gamma N \to \rho N$ cross sections, the pion cloud dressing corresponds to t-channel pion exchanges (with either nucleon or delta final states), as well as contact terms dictated by gauge invariance. The σ, f_2, and Pomeron exchanges are not included in the in-medium ρ spectral function, where they would most notably contribute at large three-momentum of the ρ meson. Because the outgoing ρ momenta in the CLAS kinematics are typically in a range around $q \simeq 1.5$–2 GeV, it is worthwhile to estimate by how much the broadening in the ρ spectral function may be underestimated at these momenta. To do this, we neglect nuclear Fermi motion and employ the schematic expression relating the total absorption cross section to the imaginary part of the in-medium ρ self-energy,

$$\Gamma_\rho = -\mathrm{Im}\Sigma_\rho/m_\rho = v_{\mathrm{rel}}\, \varrho_N\, \sigma^{\mathrm{tot}}_{\rho N}. \tag{1}$$

Assuming a (nonresonant) ρN cross section of 40 mb for a $q = 2$ GeV ρ imparting on a nucleon at rest, $v_{\mathrm{rel}} = 0.9$ and, using $\varrho_N = 0.5\varrho_0$, we find $\Gamma_\rho \simeq 60$ MeV. This is to be compared to the in-medium ρ-meson width obtained for the model employed here, amounting to $\sim$40 MeV (for $q = 2$ GeV, $\varrho_N = 0.5\varrho_0$; see, e.g., Fig. 4 in our previous article [22]). This estimate suggests that we may underestimate the ρ width at high momenta by up to 20 MeV.[1]

With reasonable control over the elementary ρ-production amplitude on the nucleon, we applied the above-constructed model to dilepton invariant-mass spectra off nuclei as measured by the CLAS Collaboration. The basic assumption in this approach is that the dilepton production process can be "factorized" into a two-step process, namely, ρ production on a single nucleon followed by its in-medium propagation and final decay. The pertinent mass-differential cross section for a fixed incoming photon energy is then given by

$$\begin{aligned}
&\left\langle \frac{d\sigma}{dM} \right\rangle_A (E_\gamma, M) \\
&= \frac{m_N^2 M}{(2\pi)^2 \varrho_A} \int \frac{d^3p}{(2\pi)^3} \frac{d^4q}{(2\pi)^4} \frac{d^4p'}{(2\pi)^4} \frac{e^2 g^2}{(k^2)^2 m_\rho^4} \\
&\quad \times \frac{[-\mathrm{Im}\Sigma^{\mathrm{vac}}_{\gamma\to e^+e^-}(q)]}{2\sqrt{(p\cdot k)^2}} \delta(q^2 - M^2) \delta\left(p'^2 - m_N^2\right) \\
&\quad \times \delta^4(k + p - q - p') \Theta(k_F - |\vec{p}|) \Theta(|\vec{p}'| - k_F) \\
&\quad \times \sum_{m_s, m_{s'}, \lambda} T^\mu(k, p, q) [T^\nu(k, p, q)]^\dagger \\
&\quad \times \left\{ P^L_{\mu\nu}(q) \left| G^L_\rho(q) \right|^2 + P^T_{\mu\nu}(q) \left| G^T_\rho(q) \right|^2 \right\},
\end{aligned} \tag{2}$$

with $k = (E_\gamma, \vec{k})$, $p = (E_p, \vec{p})$, $p' = (E_{p'}, \vec{p}')$, and $q = (q_0, \vec{q})$ being the four-momenta of the incoming photon, incoming nucleon, outgoing nucleon (all on-shell), and outgoing ρ (i.e., dilepton), respectively. Furthermore, T^μ is the ρ photoproduction amplitude off the nucleon, $G^{L,T}_\rho$ are the longitudinal and transverse electromagnetic correlators encoding the in-medium ρ propagator,[2] and $P^{L,T}$ are the

[1] However, smaller momenta contribute and the "average" density probed by the CLAS experiment is $\sim 0.4\varrho_0$ for ^{56}Fe targets; see also later discussion.

[2] For example, $G_\rho = (m_\rho^2/g_\rho) D_\rho$ in the vector dominance model (VDM). The present approach accounts for corrections to VDM in the baryon sector as described in Ref. [23].

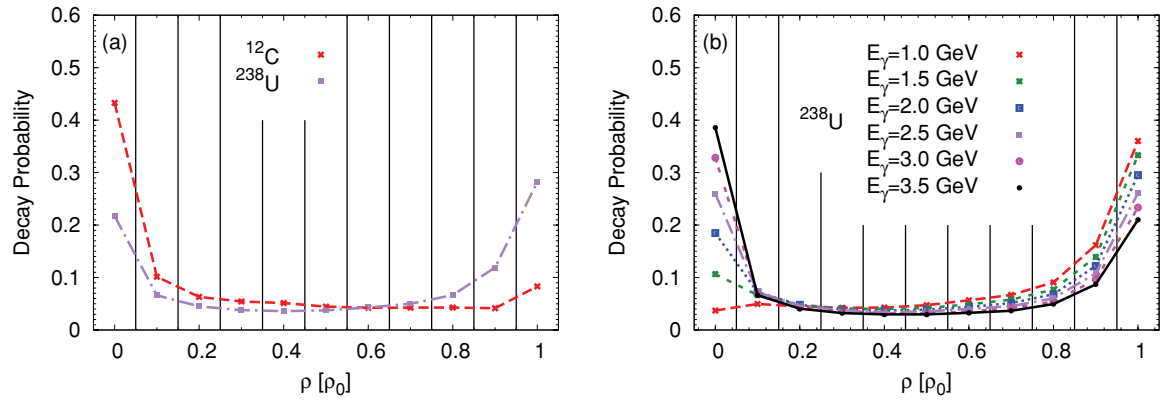

FIG. 1. (Color online) Probability distributions (normalized to 1) of the nuclear density at the ρ-meson decay points, $dP_{\rm decay}/d\varrho_N$: (a) using an input photon-energy spectrum as in CLAS for two different nuclei and (b) using a ^{238}U target for different photon energies. Vertical lines indicate the bins used for the histogram.

standard four-dimensional projection operators. As is usual in many-body theory, the in-medium width (imaginary part of the self-energy) of a particle is calculated in terms of the imaginary part of the forward scattering amplitude on particles of the medium, corresponding to absorption in the forward direction. These processes include finite-angle elastic scattering. Thus, Eq. (2) does not include the dilepton decay of ρ mesons after being scattered elastically at finite angle. There are several reasons why this contribution can be expected to be small. For example, the nucleon on which the scattering occurs is either Pauli-blocked (not for forward scattering) or ejected from the nucleus (i.e., corresponding to an extra particle in the final state). Formally, one would have to calculate such a contribution by inserting an extra ρ-N scattering amplitude into Eq. (2), together with an extra folding over a nuclear Fermi distribution of the struck nucleon. Thus, this process is formally of higher order in density. Given the fact that the in-medium part of the ρ width is basically linear in density (e.g., cf. Fig. 11 in Ref. [3]), higher orders owing to elastic finite-angle scattering should be suppressed as well. Of course, ultimately, one should compare our predictions for total dilepton production cross sections to absolutely normalized data, which, unfortunately, are not available at this point.

With a realistic photon input spectrum consisting of six bins of photon energies, $E_\gamma = 1.0$, 1.5, 2.0, 2.5, 3.0, and 3.5 GeV with relative weights of 13.7%, 23.5%, 19.3%, 20.1%, 12.6%, and 10.9%, respectively, a fairly good description of the excess mass spectra[3] for deuteron and iron targets was found [22]. For the full in-medium propagator of the ρ encoded in G_ρ, the input density has to be specified. In Ref. [22] this was done rather schematically by evaluating an average density at the ρ's final decay point, implying that the ρ-meson propagator quickly relaxes to the surrounding medium. The (average) density at the decay point was estimated assuming (i) a Woods-Saxon profile for the nucleus, (ii) a uniform sampling of the nucleus for the production point (i.e., the incoming photon reacts equally likely with each nucleon), and (iii) a ρ-meson path length, collinear with the incoming photon momentum and estimated using an average ρ momentum of $q \simeq 2$ GeV (determining its velocity), and an average in-medium ρ lifetime of $\bar{\tau}_\rho = 1/\bar{\Gamma}^{\rm med} = 1/200$ MeV $=$ 1 fm/c. The resulting average density for ^{56}Fe turned out to be $\sim 0.5\varrho_0$, but the variations in the normalized spectra are small when varying this density within $\pm 0.1\varrho_0$. (Note that, at these densities and three-momenta, the width of the microscopic spectral function is indeed around 200 MeV, which is consistent with the average lifetime used for the density estimate.)

Here we improve upon the above procedure in several respects. First, the width, and thus the decay time, of the ρ meson depends on its three-momentum. We replace the average value used before with the explicit momentum dependence given by our microscopic model for the propagator. In particular, slow ρ mesons decay faster than fast ones that consequently travel farther. This could be significant in view of the rather large range of photon energies (between 0.6 and 3.8 GeV) as used by the CLAS Collaboration [24]. Second, the assumption that all ρ mesons of a given velocity decay after a fixed (average) travel distance, L, is subject to corrections. Here we include the exponential decay characteristics as

$$\frac{dN}{dt} = \exp(-\Gamma[\varrho_N(\vec{r}), v]t), \tag{3}$$

implying that even for identical kinematics and production point the path length varies and thus different densities at the decay point are probed. The initial creation points of the ρ meson are still distributed according to a realistic density profile for each nucleus [25] (weighted by volume). Following this procedure we obtain the decay points and thus a distribution determining how many ρ mesons decay at a given density. The final spectrum then follows, using this distribution in the electromagnetic correlator (rather than an average density).

In Fig. 1 we show the resulting distributions of ρ-decay points as a function of nuclear density, for a small and a large nucleus integrated over the initial photon energy spectrum as specified above [Fig. 1(a)], and for a heavy nucleus resolved

[3]An "excess" mass spectrum is defined as the signal spectrum (after combinatorial background subtraction) with the (narrow) ω and ϕ peaks subtracted. The remaining signal is then associated with the ρ-decay contribution.

into different initial photon energies [Fig. 1(b)]. In both distributions we observe a clustering of the decay points at the low and high ends of the available densities. In particular, the absolute maximum shifts from the lowest density bin ($\varrho_N \simeq 0$) for small nuclei to the highest one ($\varrho_N \simeq \varrho_0$) in heavy nuclei, and similarly when going from high to low photon energies. The two-hump structure of the distributions reflects the rather sharp transition in the nuclear density profiles from a dense interior to the vacuum, with a relatively thin surface layer. For the CLAS input photon spectrum (which ultimately determines the ρ's velocity and the time dilation of its decay time), the use of a heavy nucleus (^{238}U) compared to a light one (^{12}C) makes a big difference, by increasing the interior decay fraction by a factor of $\sim$3 while decreasing the outside decays by a factor of $\sim$2 [see Fig. 1(a)]. Reducing the photon energy is particularly efficient in suppressing outside decays [see Fig. 1(b)], while the exponential decay characteristics induce a good fraction of interior decays for relatively fast ρ mesons. The asymmetries in the densities of the decay points are the main difference compared to the use of an average density in our earlier work [22], which is at the origin of the slight variation in the results shown below.

III. SIGNATURES OF MEDIUM EFFECTS

In Sec. III A we first discuss the updated inclusive dilepton mass spectra in comparison to the CLAS data, as following from the improved evaluation of decay-point densities as described in the previous section. In Secs. III B–III D, we then scrutinize the origin of the medium effects to identify observables that can improve our understanding of the medium effects and test consistency of spectral shapes and absolute yields.

A. Update of invariant-mass spectra and comparison to CLAS data

In Fig. 2 we compare our earlier calculations for the ^{56}Fe target with our improved calculation and with the CLAS data at JLab [15,16]. It also includes the comparison for the ^{12}C target. The average densities of $0.3\varrho_0$ for carbon and $0.4\varrho_0$ for iron correspond to the averages obtained from the density distributions in the improved scheme. (As we see in Sec. III D, such averages are also estimated from the transparency ratios for total cross sections.) One finds that the inclusion of the explicit density distribution leads to a small downward shift of the ρ-resonance peak in the spectrum, which improves the description of the data compared to the calculation using an average density. The reason for this effect is that ρ mesons with large momentum, which predominantly figure into the high-mass part of the spectrum, now effectively decay at lower densities, implying reduced medium effects, that is, a narrower distribution (and a slightly smaller upward mass shift). This suppresses the high-mass tail of the dilepton spectrum and increases the peak height. Overall, the full model gives a good description of the data for both nuclei and provides a

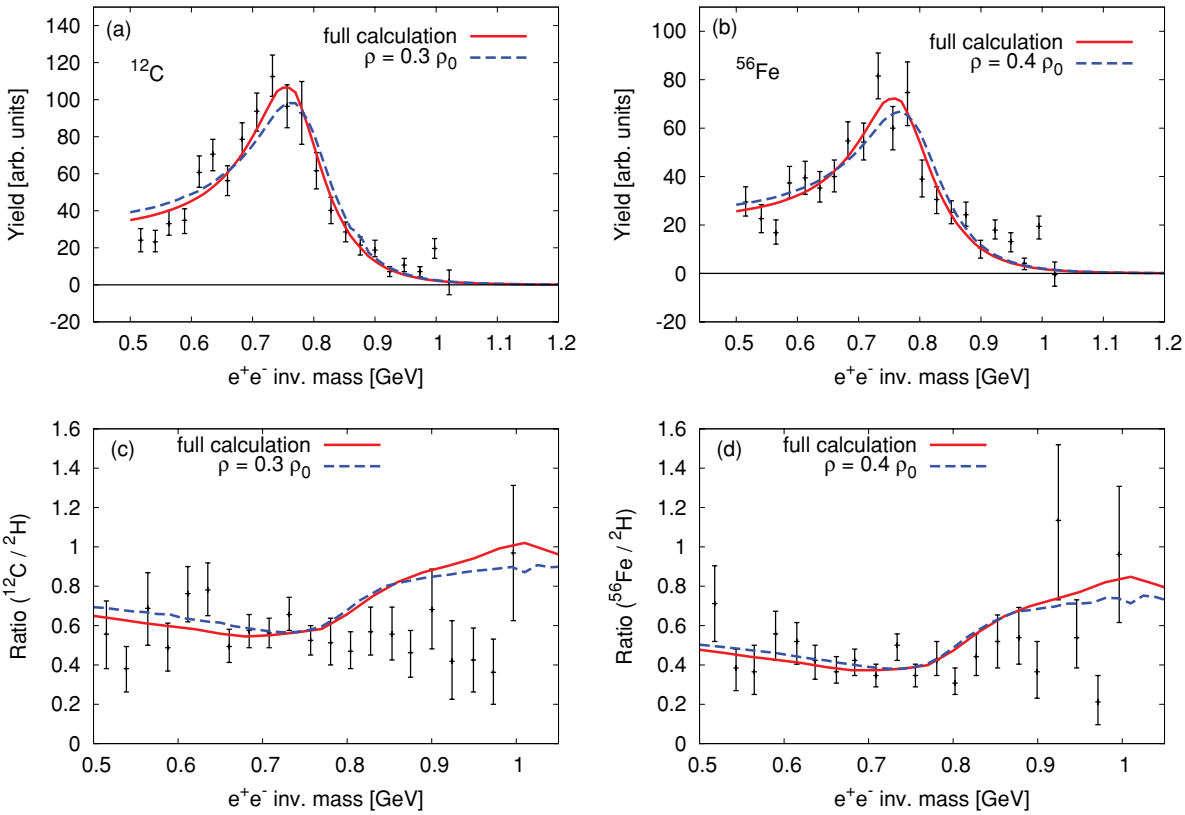

FIG. 2. (Color online) Excess mass spectra for (a) ^{12}C and (b) ^{56}Fe and (c, d) ratios of these spectra to the deuterium spectrum. (In the ratios, both numerator and denominator are normalized to the corresponding target-mass number, A.) The full calculation using explicit density distributions (solid lines) is compared to simplified calculations using a single average density.

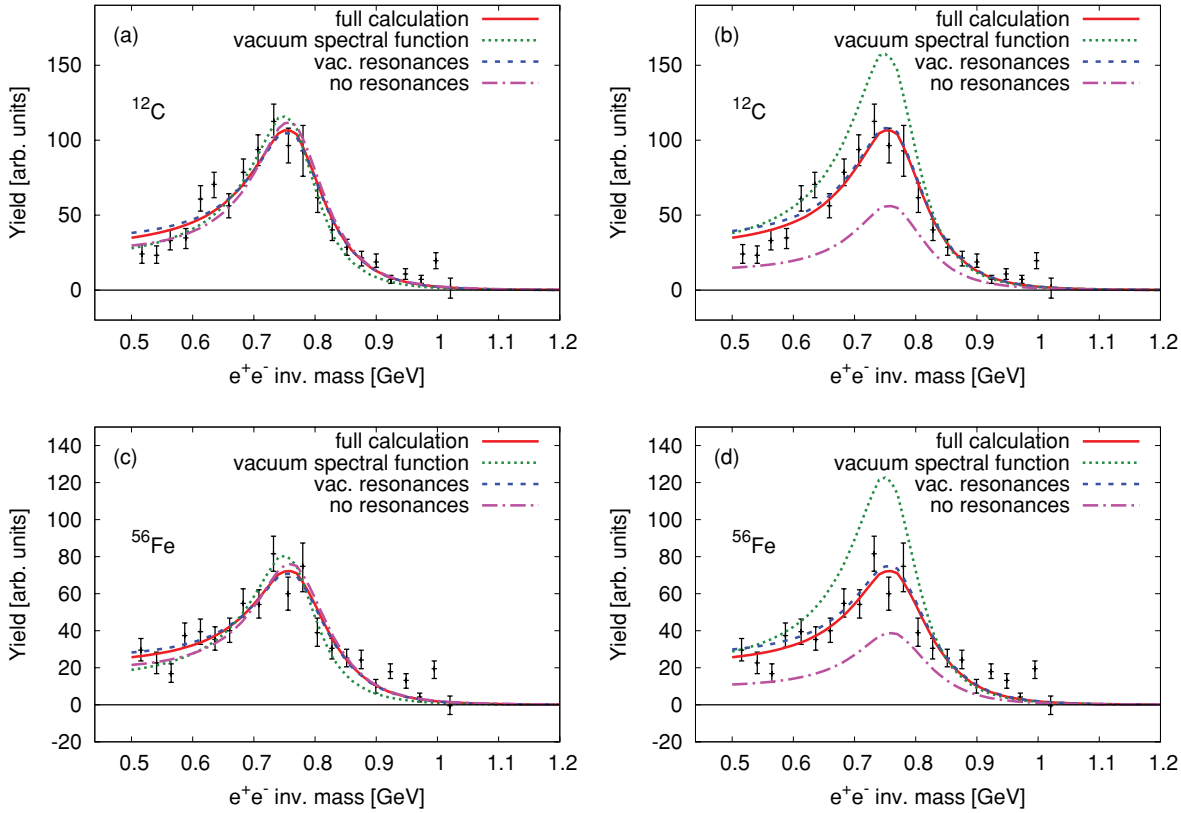

FIG. 3. (Color online) Calculations for excess mass spectra off (a, b) ^{12}C and (c, d) ^{56}Fe targets compared to the CLAS data [15,16] at JLab. The full calculations (solid lines) are decomposed by modifying different theoretical ingredients, by (i) switching off the baryon-resonance contributions in the elementary production amplitude (dash-dotted lines), (ii) switching off the in-medium widths of the baryon-resonance contributions in the elementary production amplitude (dashed lines), or (iii) replacing the in-medium electromagnetic correlator, G_ρ, with the vacuum one (dotted lines). (a, c) All spectra are (χ^2) normalized to the data, while (b, d) we keep the normalization of the full model also for the other scenarios.

reasonable baseline for an advanced analysis of in-medium effects. We note that our findings are in good agreement with the results of the Boltzmann-Uehling-Uhlenbeck (BUU) transport simulations by the Giessen group [16,18,26] based on the spectral function of Ref. [12]. Also in this calculation, a broadening of the ρ-meson spectral function by $\sim$70 MeV was found without significant mass shift.

Next, we address the influence of different model components on the shape and magnitude of the invariant-mass spectra. In Fig. 3, we display the results of the calculations in which (i) the resonances in the production amplitude are switched off (dash-dotted lines), (ii) the resonances in the production amplitude are kept as in the vacuum (i.e., without in-medium broadening as specified in Refs. [1,23]; dashed lines), and (iii) the vacuum propagator for the ρ meson is employed (dotted lines). In Figs. 3(a) and 3(c), the integrated yield for each scenario is normalized to the experimental data (which to our knowledge are not absolutely normalized) using a χ^2 fit.[4] In Figs. 3(b) and 3(d), only the full calculations (solid lines) are (χ^2) normalized to the data and the same normalization factor is then applied to all other curves, which maintains the relative normalization of all theory curves. The following observations are made. The impact of the in-medium broadening of the baryon resonances on the production amplitude is essentially negligible, in both the shape [Figs. 3(a) and 3(c)] and absolute magnitude [Figs. 3(b) and 3(d)] of the final dilepton spectra. Switching off the resonance contributions in the production amplitude altogether (dash-dotted lines) leads to a slight narrowing of the spectral shape [Figs. 3(a) and 3(c)] but, more significantly, reduces the absolute yield of the cross section by more than 50% [see dash-dotted lines in Figs. 3(b) and 3(d)]. This can be easily understood since the resonances play a significant role in the total ρ photoproduction cross section on the nucleon for photon energies below $E_\gamma \simeq 2$ GeV [22]. An important question concerns the sensitivity of the spectra to the medium effects in the ρ-meson propagator. We investigate this question by replacing the in-medium propagator with the vacuum one (resulting in the dotted lines in Fig. 3). The spectral shape narrows, but not as much as one may have expected. In fact, when normalizing the theory curves to the experimental data, the resulting spectral shapes for vacuum and in-medium correlators are not much different for both carbon and iron targets [see Figs. 3(a) and 3(c)]. More quantitatively, for the carbon target, the χ^2 per data point is close to 1 for both

[4]Alternatively, one could normalize to the integrated strength of the spectrum. The differences in both procedures are negligible.

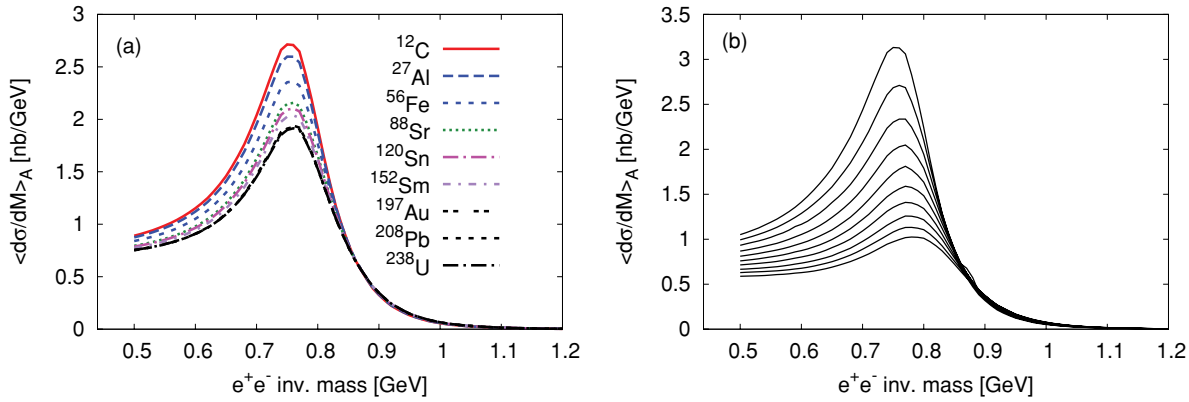

FIG. 4. (Color online) Absolutely normalized cross sections for excess mass spectra for (a) several nuclei from carbon (uppermost curve) to uranium (lowest curve) and for (b) several fixed nuclear densities from $0.1\varrho_0$ (uppermost curve) to ϱ_0 (lowest curve).

in-medium and vacuum ρ propagator; that is, no significant distinction can be made. For the iron target, we actually have a preference of 1.08 over 1.55 in the χ^2 when using the in-medium propagator. This is in line with the analyses carried out in Ref. [16] based on BUU calculations [18,26] with the in-medium broadened spectral function of Ref. [12], or on direct fits to the spectra with a Breit-Wigner ansatz for the spectral function [16]. We recall that the absolute yields of the spectra markedly increase for the vacuum spectral function compared to the in-medium one (which is more systematically quantified in Sec. III D).

The question we want to address in the following is how we can better discriminate medium effects from the experimental data. For example, for the many-body spectral function employed in our approach, the broadening is much more pronounced at low three-momenta (relative to the nuclear rest frame). The moderate broadening observed in the CLAS data is accounted for by the reduced medium effects at large three-momentum (following from the relatively soft hadronic form factors as determined in Refs. [1,23]), as well as the limited fraction of in-medium decays even for the iron target. We investigate several ways to better pin down medium effects. First, one could use heavier nuclei. This would allow more ρ mesons to decay inside the nucleus and thus augment the medium effects [recall Fig. 1(a)]. In addition, the density dependence of the spectral function could be studied. Second, one could concentrate on lepton pairs with low three-momentum, which should enhance the decay fraction inside the nucleus because of the smaller distance they travel from production to decay point.[5] A breakdown of the data in several momentum bins would illuminate the three-momentum dependence of the spectral function, a critical property as indicated above. Third, as the presumably most straightforward option on the experimental side, one could utilize the absolute magnitude of the total cross section in terms of the so-called nuclear transparency ratio.

[5]This poses formidable experimental challenges because in the present CLAS setup only a detection of pairs with momenta above ∼1 GeV is feasible [4].

The above-listed three possibilities are elaborated in Secs. III B, III C, and III D, respectively. To facilitate direct comparisons to (existing or future) CLAS data, we use the same folding over the incoming photon-energy spectrum as quoted above [24], unless stated otherwise. Our hope is that several long-standing issues about basic properties of the ρ-spectral function in nuclear matter (see, e.g., the differences between the spectral functions of Refs. [10,12,13,27]) could be resolved by detailed studies of accurate e^+e^- spectra in reactions off nuclei. One of our main goals is to quantify the notion of "accurate."

B. Dependence of the spectral shape on A

A systematic study of the A dependence of the absolutely normalized dilepton mass spectra under the CLAS conditions is compiled in Fig. 4(a). One clearly recognizes the enhanced sensitivity to the medium effects with increasing A of the nucleus, mostly owing to the simple fact that a larger nuclear volume increases the fraction of in-medium decays (recall also Fig. 1). The "gain" in medium effects is quite appreciable when going from the currently available iron target to Au, Pb, or U, which is more pronounced than the difference between C and Fe. It instructive to compare the A dependence of the spectra to the density dependence in infinite nuclear matter, as shown in Fig. 4(b). This comparison suggests that, for $A \simeq 200$ targets, the inclusive spectral shape (or net broadening) corresponds to rather moderate average densities, $\bar{\varrho}_N \simeq 0.5\varrho_0$. In an attempt to better quantify the sensitivity of the spectral shape to the in-medium broadening, we compare in Fig. 5 the full calculations (solid lines) with calculations using the vacuum spectral function, where the latter are normalized such that the peak height coincides with the full calculation for each of the four nuclei. The sensitivity to medium effects may then be defined as the enhancement of the full over the vacuum curve in the low-mass tail (e.g., at $M = 0.5$ GeV). The pertinent low-mass enhancement factors are 1.35, 1.49, 1.6, and 1.73 for $A = 12$, 56, 120, and 238, respectively.

C. Three-momentum dependence

Next we investigate the option of applying three-momentum cuts on the outgoing lepton pair (which in our

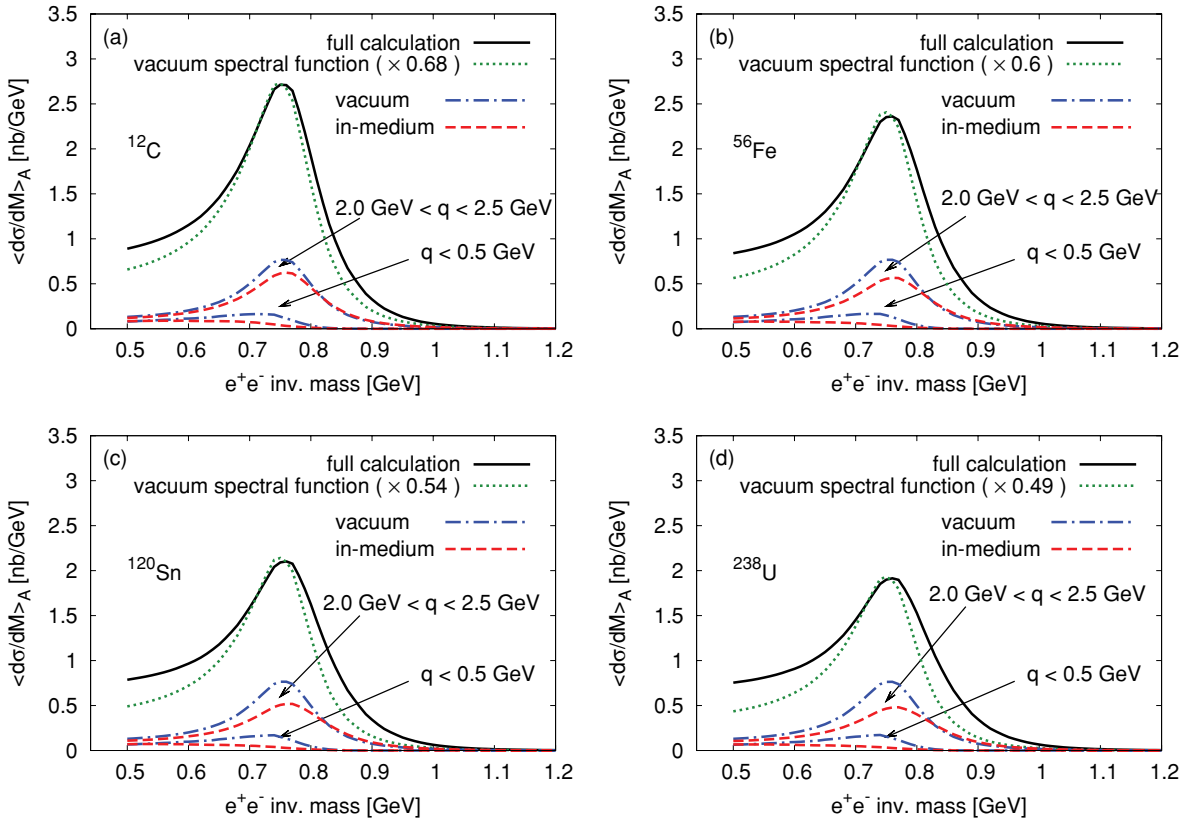

FIG. 5. (Color online) Excess dilepton invariant-mass spectra for several nuclei. The full model (solid lines) is compared to the calculations using the vacuum ρ propagator (scaled to the peak height of the full calculation by the indicated factors). Furthermore, absolutely normalized calculations are shown for in-medium and vacuum spectral functions applying the indicated momentum cuts to the spectra.

approximation is equivalent to the three-momentum of the ρ relative to the nuclear rest frame). From general considerations (and our discussions in Sec. II), we expect that low-momentum dilepton samples should contain noticeably larger fractions of ρ decays in the nuclear volume. Figure 5 contains the results where the three-momentum of the outgoing ρ is restricted to lie either below 0.5 GeV or between 2.0 and 2.5 GeV. We refer to the former as "low-momentum cut," while the latter represents a typical momentum range resulting from the photon input spectrum used by the CLAS Collaboration (this range of "intermediate" momenta accounts for roughly 25% of the total yield for the full calculation). The potential benefits of a low-momentum cut are twofold. In addition to the already mentioned increase of decay probability in the nuclear volume (which also augments the decays at higher densities), the medium modifications of our ρ spectral functions increase appreciably toward smaller momenta. The numerical results displayed in Fig. 5 corroborate the discrimination power of the low-momentum cut. The shape of the resulting mass spectrum is markedly different when the full calculation (dashed lines) is compared with a calculation where the vacuum propagator is used instead (dot-dashed lines), already for rather light nuclei. The main effect is a quenching of the ρ peak at its resonance position, while the (absolute values of the) low-mass cross section turn(s) out to be very similar (the absorption is approximately compensated by the spectral broadening). Again, one may try to quantify the sensitivity to the medium effects by defining an appropriate ratio. The coincidence of the low-mass cross section suggests the peak ratio as a suitable measure, that is, the ratio of the resonance peak for the vacuum calculation to the value at the same mass for the full calculation. For the low-momentum (high-momentum) cut we find ratios of 2.4 (1.2), 2.8 (1.4), 4.2 (1.5), and 4.4 (1.6) for $A = 12$, 56, 120, and 238, respectively, which provides a much more increased sensitivity over the inclusive shape analysis. Indeed, when comparing the cross sections for vacuum and in-medium spectral functions for the above defined "representative" three-momentum range, the sensitivity is substantially reduced.

D. Transparency ratio (yield)

Finally, we turn to our third option to scrutinize medium effects, by studying the absorption of ρ mesons rather than the spectral shape of the dilepton invariant-mass spectra. The width figuring into the mass spectra is of the same physical origin as the forward absorption of ρ mesons when traveling through the nuclear medium. Experimentally, the nuclear absorption is usually quantified by the nuclear transparency ratio,

$$T_A = \frac{\sigma_{\gamma A\to\rho X}}{A\sigma_{\gamma N\to\rho X}} \simeq \frac{\int dM \langle d\sigma/dM\rangle_{\rm med}}{\int dM \langle d\sigma/dM\rangle_{\rm vac}}, \qquad (4)$$

which measures the suppression of the nuclear cross section per nucleon, relative to the cross section on the

free nucleon (note that the latter cross section includes the finite decay width of the ρ in vacuum). This quantity was previously measured in nuclear photoproduction of ω and ϕ mesons [28–30], from which large in-medium widths of $\sim$100–150 MeV were extracted (see also Refs. [26,31,32] for theoretical evaluations). These values are more than an order of magnitude larger than the respective vacuum widths of ω ($\Gamma_\omega = 8.5$ MeV) and ϕ ($\Gamma_\phi = 4.3$ MeV). This is the main reason why for narrow vector mesons the transparency ratio is much more sensitive to medium effects than invariant-mass spectra (in which the in-medium to vacuum decay fraction is small). The transparency ratio is less favorable for the ρ meson, where the large vacuum width suppresses the contribution from vacuum decays (which, in principle, is of course a welcome feature). In addition, the integration ranges in the transparency ratio, Eq. (4), become more ambiguous for a broad resonance, at least in practice (i.e., in experiment). However, we already deduced from Fig. 3 that, also for the ρ meson, the change in the absolute yields may be more pronounced (i.e., easier to observe) than the medium modifications of the spectral shape, at least for relatively small nuclei and toward higher momentum. We therefore computed the nuclear transparency ratio for the ρ meson within our approach[6] by integrating the invariant-mass spectra as computed above over $M = 0.5$–1.1 GeV. The results are displayed in Fig. 6 as a function of nuclear mass number A. Even for small nuclei a considerable suppression occurs, which gradually becomes stronger for larger nuclei until a ratio of about 0.6 is reached for uranium. This is to be compared to the measurements for the ϕ and ω, where the suppression reaches down to $\sim$0.4, even when normalizing to carbon. Again, the reason for the apparently weaker effect for ρ is its large vacuum width of $\sim$140 MeV, relative to which changes in the medium are at most a factor of 2–3. On the contrary, for ω and ϕ, more than a factor of 10 broadening was extracted and/or predicted [11,33–38], which leads to much stronger effects in the transparency ratio. For completeness, we also investigated different components in our model calculation. When leaving out the in-medium width increase of the baryon resonances in the production amplitude, T_A exhibits a small enhancement of about 0.025–0.05 owing to a small increase in the production cross section. This effect was essentially invisible at the level of the invariant-mass spectra and underlines the sensitivity of the transparency ratio to even small variations in the calculation. The main suppression mechanism is, as expected, caused by the absorption of the propagating ρ meson, as illustrated by using the vacuum propagator in which case T_A is close to 1 (the small residual suppression being caused by the medium modifications in the production cross section, essentially due to the in-medium width of the resonances).

[6]Note that our spectra shown above were already normalized per nucleon [22] so that no extra factor A should be included.

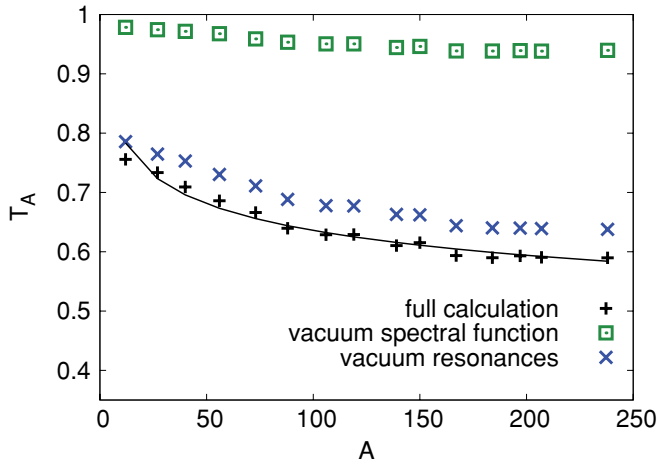

FIG. 6. (Color online) Nuclear transparency ratio, T_A, as a function of nuclear mass number, A. The full calculation is compared to results when switching off the medium effects on the baryon resonances in the production amplitude and when using the vacuum ρ propagator in the electromagnetic correlator, G_ρ.

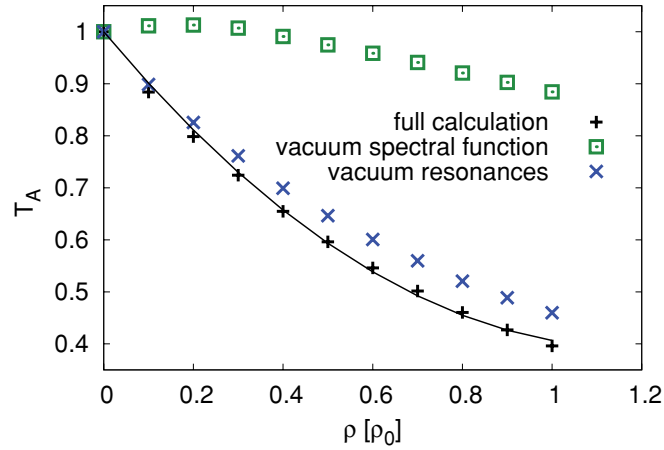

FIG. 7. (Color online) Same as Fig. 6 but in infinite nuclear matter as a function of density.

It is instructive to evaluate the nuclear transparency ratio as a function of nuclear density in infinite nuclear matter[7] (cf. Fig. 7). This enables yet another angle at the question of what typical ("average") densities might be representative for a given nucleus. For example, we find that to obtain the same T_A for ^{12}C (^{56}Fe) an infinite-matter density of about 0.2–0.3ϱ_0 (0.3–0.4ϱ_0) should be used, which is consistent with the values obtained with the method used in Ref. [22].

Of further practical interest is the dependence of T_A on the incoming photon energy. This information is displayed for our approach in Fig. 8, which shows that the suppression markedly increases with decreasing photon energy. Lower photon energies produce ρ mesons of smaller three-momentum, which in turn increases the time spent in the nuclear medium and thus provides longer durations of suppression. In fact, for incoming photon energies below $E_\gamma \simeq 1.5$ GeV, directed onto $A \simeq 200$ targets, T_A has approached the infinite-matter value for saturation density (0.4) within about 20%. This reiterates

[7]Note that we apply the notion of "infinite matter" only to the strong-interaction parts of the calculation; i.e., we still pretend that the medium remains transparent to the electromagnetic probe so that dileptons can leave without reinteractions.

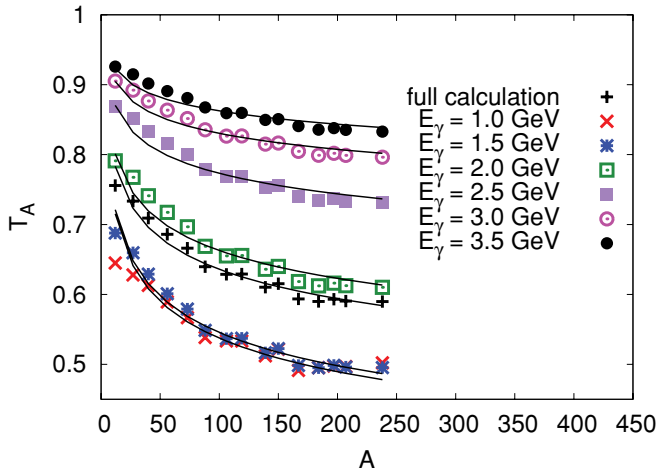

FIG. 8. (Color online) Transparency ratio as a function of the mass number A for different photon energies.

once more the power of low-momentum cuts on the lepton pair. To quantify the A dependence of the transparency ratio in a functional form, we fitted our results in Figs. 6 and 8 with the standard power-law ansatz, $T_A = A^\beta$. For the individual incoming photon energies, the extracted values of β are plotted in Fig. 9. For the full calculation using the weighted input spectrum corresponding to the JLab beam, we find a value of $\beta = -0.0983$. Its magnitude is significantly smaller than for the available ω and ϕ data, but, surprisingly, is comparable to J/ψ suppression in fixed-target p-A collisions at high energy. (See, e.g., the recent compilation in Ref. [39] where the exponent $\alpha \equiv 1 + \beta$; however, this is most likely a coincidence since the physics of ρ and J/ψ nuclear suppression is presumably quite different.) Note that the overall β value for the incoming photon spectrum would correspond to an "average" photon energy of slightly below $E_\gamma = 2$ GeV (the weighted mean of our input distribution is $\bar{E}_\gamma = 2.14$ GeV). We finally remark that, especially for light nuclei like carbon, a more complicated fit function would be required to accurately reproduce the calculated values of T_A.

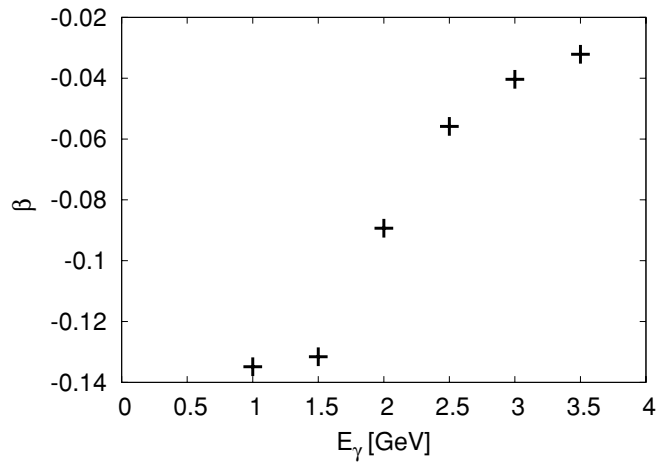

FIG. 9. Fit parameter β used to describe the dependence of the transparency ratio on the photon energy.

IV. CONCLUSIONS

We conducted a theoretical analysis of invariant-mass spectra and total cross sections of dileptons in nuclear photoproduction for incoming photon energies in the few-GeV regime as recently measured by the CLAS Collaboration at JLab. Our approach is based on an effective hadronic model in which we combined in a consistent way an earlier constructed elementary production amplitude with an in-medium ρ propagator. The former describes well the ρ production off the nucleon, while the latter was successfully applied to dilepton spectra measured in high-energy heavy-ion collisions at the CERN-SPS.

We first improved on our earlier calculations [22] by constructing a more realistic density distribution for the decay points of the ρ meson which, in particular, accounts for the three-momentum dependence of the nuclear path length in connection with the microscopic in-medium width in the propagator. This leads to a slight improvement in the description of the invariant-mass spectra measured by the CLAS Collaboration for iron targets, which we also extended to carbon targets. The sensitivity to medium effects in the inclusive mass spectra is, however, somewhat limited in the absence of absolutely normalized data. Calculations for heavier target nuclei indicate that the situation improves when increasing the nuclear-mass number to $A \simeq 200$. A more powerful lever arm turns out to be a cut on the outgoing lepton pair momentum. For small momenta, say, $q \leqslant 0.5$ GeV, the spectral shape becomes very flat with hardly any ρ resonance peak left. The reason for this effect is twofold: the kinematics make slow ρ mesons stay longer in the nuclear volume and thus enhance the in-medium decay fraction; but dynamics cause the medium effects in the ρ spectral function to increase substantially toward small three-momentum. It is this dynamic effect that reconciles the large medium effect observed in heavy-ion collision (average ρ width of ~350–400 MeV [9] as extracted from the NA60 data on low-mass dimuons) with the rather moderate modifications ($\Gamma_\rho \simeq 220$ MeV from the current CLAS data) in nuclear photoproduction. This clearly calls for a low-momentum measurement in the latter experiments, to scrutinize the three-momentum dependence of the medium effects as well as the prevalence of baryon-induced modifications in the interpretation of the dilepton data in ultrarelativistic heavy-ion collisions. We furthermore found that the nuclear dependence of absolute production cross sections can be used as a rather sensitive, complementary measure for the in-medium width. These are conveniently analyzed using the so-called nuclear transparency ratio. While the sensitivity to an increase in the absolute value of the width is less pronounced for ρ than for the narrow vector mesons ω and ϕ, we still predict a substantial reduction of this ratio, which should be straightforward to measure. An important point here is that, for ρ, the yield measurements can be effectively combined with, and tested against, the spectral information from the invariant-mass distributions (which is very challenging for the narrow vector mesons owing to their large decay fraction outside the nuclear volume).

As a further direct extension of the present work, we plan to study dilepton spectra in nuclear electroproduction

(via the reaction $e^- A \to e^- e^+ e^- A$), which would provide further constraints by investigating the various mechanisms discussed in this article under modified kinematics. It would also be interesting to study $\pi^+\pi^-$ final states, which are more easily accessible experimentally [40] but suffer from extra absorption factors on the outgoing pions, thus reducing the sensitivity to the central densities in nuclei. It would be very illuminating to perform detailed comparisons to transport theoretical calculations. The latter, in principle, perform a better treatment of the off-equilibrium aspects in the propagation process, whereas the implementation of broad spectral functions is more involved than in equilibrium approaches like the one adopted here. A continued effort on both experimental and theoretical fronts, in both heavy-ion and nuclear production contexts, holds exciting prospects for further progress in the understanding of hadron properties in the medium.

ACKNOWLEDGMENTS

We are grateful to C. Djalali for fruitful discussions. F.R. and R.R. were supported by the US National Science Foundation through CAREER Grant No. PHY-0449489. T.-S.H.L. was supported by the US Department of Energy, Office of Nuclear Physics Division, under Contract No. DE-AC02-06CH11357.

[1] R. Rapp and J. Wambach, Adv. Nucl. Phys. **25**, 1 (2000).
[2] R. S. Hayano and T. Hatsuda, (submitted to Rev. Mod. Phys.), arXiv:0812.1702 [nucl-ex].
[3] R. Rapp, J. Wambach, and H. van Hees, in *Relativistic Heavy-Ion Physics*, edited by R. Stock and Landolt-Börnstein (Springer), New Series I/23-A (2010), 4-1, arXiv:0901.3289 [hep-ph].
[4] S. Leupold, V. Metag, and U. Mosel, Int. J. Mod. Phys. E **19**, 147 (2010).
[5] R. Arnaldi *et al.* (NA60 Collaboration), Phys. Rev. Lett. **96**, 162302 (2006).
[6] D. Adamova *et al.* (CERES/NA45 Collaboration), Phys. Lett. B **666**, 425 (2008).
[7] I. Tserruya, in *Relativistic Heavy-Ion Physics*, edited by R. Stock and Landolt-Börnstein (Springer), New Series I/23-A (to be published), arXiv:0903.0415 [nucl-ex].
[8] R. Arnaldi *et al.* (NA60 Collaboration), Eur. Phys. J. C **59**, 607 (2009).
[9] H. van Hees and R. Rapp, Nucl. Phys. A **806**, 339 (2008).
[10] R. Rapp and J. Wambach, Eur. Phys. J. A **6**, 415 (1999).
[11] V. L. Eletsky, M. Belkacem, P. J. Ellis, and J. I. Kapusta, Phys. Rev. C **64**, 035202 (2001).
[12] M. Post, S. Leupold, and U. Mosel, Nucl. Phys. A **689**, 753 (2001).
[13] D. Cabrera, E. Oset, and M. J. Vicente Vacas, Nucl. Phys. A **705**, 90 (2002).
[14] M. Naruki *et al.*, Phys. Rev. Lett. **96**, 092301 (2006).
[15] R. Nasseripour *et al.* (CLAS Collaboration), Phys. Rev. Lett. **99**, 262302 (2007).
[16] M. H. Wood *et al.* (CLAS Collaboration), Phys. Rev. C **78**, 015201 (2008).
[17] G. M. Huber *et al.* (TAGX Collaboration), Phys. Rev. C **68**, 065202 (2003).
[18] M. Effenberger, E. L. Bratkovskaya, and U. Mosel, Phys. Rev. C **60**, 044614 (1999).
[19] M. Schafer, H. C. Donges, and U. Mosel, Phys. Lett. B **342**, 13 (1995).
[20] M. F. M. Lutz and M. Soyeur, Nucl. Phys. A **760**, 85 (2005).
[21] Y. Oh and T.-S. H. Lee, Phys. Rev. C **69**, 025201 (2004).
[22] F. Riek, R. Rapp, T.-S. H. Lee, and Y. Oh, Phys. Lett. B **677**, 116 (2009).
[23] R. Rapp, M. Urban, M. Buballa, and J. Wambach, Phys. Lett. B **417**, 1 (1998).
[24] C. Djalali (CLAS Collaboration) (private communication).
[25] H. De Vries, C. W. De Jager, and C. De Vries, At. Data Nucl. Data Tables **36**, 495 (1987).
[26] P. Muhlich, T. Falter, C. Greiner, J. Lehr, M. Post, and U. Mosel, Phys. Rev. C **67**, 024605 (2003).
[27] M. F. M. Lutz, G. Wolf, and B. Friman, Nucl. Phys. A **706**, 431 (2002).
[28] T. Ishikawa *et al.*, Phys. Lett. B **608**, 215 (2005).
[29] M. Kotulla *et al.* (CBELSA/TAPS Collaboration), Phys. Rev. Lett. **100**, 192302 (2008).
[30] R. Nasseripour, C. Djalali, M. Wood, and D. Weygand, AIP Conf. Proc. **1056**, 223 (2008).
[31] P. Muhlich and U. Mosel, Nucl. Phys. A **773**, 156 (2006).
[32] M. Kaskulov, E. Hernandez, and E. Oset, Eur. Phys. J. A **31**, 245 (2007).
[33] F. Riek and J. Knoll, Nucl. Phys. A **740**, 287 (2004).
[34] G. Wolf, B. Friman, and M. Soyeur, Nucl. Phys. A **640**, 129 (1998).
[35] P. Roy, S. Sarkar, Jan-e Alam, B. Dutta-Roy, and B. Sinha, Phys. Rev. C **59**, 2778 (1999).
[36] F. Klingl, N. Kaiser, and W. Weise, Nucl. Phys. A **624**, 527 (1997).
[37] R. Rapp, Phys. Rev. C **63**, 054907 (2001).
[38] B. Kämpfer and S. Zschocke, Prog. Part. Nucl. Phys. **53**, 317 (2004).
[39] R. Rapp, D. Blaschke, and P. Crochet, (submitted to Prog. Part. Nucl. Phys.), arXiv:0807.2470.
[40] S. A. Morrow *et al.*, Eur. Phys. J. A **39**, 5 (2009).